

Fluorescence of RbH and RbD Formed by Irradiating the Mixed Gases Rb+H₂ and Rb+D₂ with Laser Light

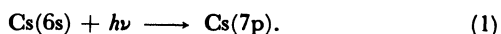
Hajime KATÔ,* Yukiko TOYOSAKA, and Tomonari SUZUKI

Department of Chemistry, Faculty of Science, Kobe University, Nada-ku, Kobe 657

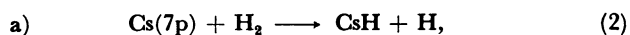
(Received August 22, 1984)

When a mixture of ⁸⁵Rb, ⁸⁵Rb₂, and D₂ was irradiated by laser light at 5145 or 4880 Å, small visible particles appeared and the fluorescence spectra were observed. By analyzing these spectra, we determined the rotational constants *B*_v and the centrifugal distortion constants *D*_v and *H*_v for the *X* ¹Σ⁺ and *A* ¹Σ⁺ states of ⁸⁵RbD. By considering the isotopic dependence of the Dunham coefficients, we determined various molecular constants of ⁸⁵RbH whose values were in good agreement with the observed fluorescence spectra of ⁸⁵RbH excited by laser lines at 4762, 4765, and 4880 Å. The process of RbH formation is discussed.

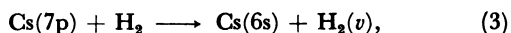
In 1975, Tam, Moe, and Happer reported that micron-size visible particles were produced in a cell filled with cesium and hydrogen upon Ar⁺-laser irradiation at 4545 or 4579 Å.¹⁾ The pressure broadening of the 7p→6s doublets at 4555 and 4593 Å allowed a substantial pumping of the Cs atoms from the ground state 6s ²S_{1/2} to the 7p ²P_{3/2} or 7p ²P_{1/2} state



They suggested that the particles (often called "laser snow") were crystals of cesium hydride salt produced by the following reactions:



or



where H₂(*v*) represents a vibrationally excited hydrogen molecule.

b) Collisions with other CsH molecules lead to a (CsH)₂ molecule, which would further polymerize to form crystals of CsH. Particle formation was also observed when rubidium, mixed with H₂, was irradiated at 4880 or 4765 Å. In this case, the first step in the process was the production of excited Rb₂ (*C* ¹Π_u) molecules. The process regarding RbH formation is interesting.

There are few previous spectroscopic analyses of RbH. In 1939 Gaydon and Pearse²⁾ observed the *A* ¹Σ⁺→*X* ¹Σ⁺ transition of RbH in the 4680 to 6540 Å region in emission. Bartky³⁾ observed the absorption spectrum of RbD. He showed that the previous vibrational assignment of the *A* ¹Σ⁺ state of RbH had to be changed, and gave revised molecular constants for RbH. Hsieh *et al.*⁴⁾ observed the laser-induced fluorescence spectra of RbH excited by an Ar⁺ laser line at 4765 Å.

Here, we report the laser-induced fluorescence spectra of RbD excited at 5145 and 4880 Å, and of RbH excited at 4762, 4765, and 4880 Å. Since the vibrational constant ω_e of RbD is about (μ^{RbH}/μ^{RbD})^{1/2} times that of RbH (where μ^{RbD} and μ^{RbH} are the reduced masses of RbD and RbH, respectively), we observed the fluorescence lines of RbD by about (μ^{RbD}/μ^{RbH})^{1/2} times that of RbH in a given energy region. Hence, we could

determine more accurate potential curves for RbD than for RbH. We report on the rotational constants *B*_v and the centrifugal constants *D*_v and *H*_v, which are independent of the method of least squares, for the *X* ¹Σ⁺ and *A* ¹Σ⁺ states of RbD. The potential curves of the *X* ¹Σ⁺ and *A* ¹Σ⁺ states and the Franck-Condon factors of the *A* ¹Σ⁺→*X* ¹Σ⁺ transition are calculated. The fluorescence spectra of RbD excited by laser lines at 4880 and 5145 Å are compared with the calculated results. By using the isotopic dependence of diatomic Dunham coefficients, we determined the molecular constants of RbH. By referring to the potential energy curves of H₂, Rb₂, and RbH, we estimated the processes of RbH formation.

Experimental

⁸⁵Rb metal was obtained by the reduction of ⁸⁵RbCl (Oak Ridge National Laboratory, 99.78% of ⁸⁵RbCl and 0.22% of ⁸⁷RbCl). A mixture of 120 mg of ⁸⁵RbCl and 120 mg of Ca metal granules was enclosed in a breakable glass tube of 6 mm o.d. with a slender neck. It was enclosed in an exhausted Pylex glass tube of 10 mm o.d. We broke the neck of the glass tube and heated the contents to 450°C for 20 min. The heating caused the ⁸⁵Rb metal to become volatilized. This ⁸⁵Rb metal was driven into a cooler part of the tube and was sealed off.

The optical cells were constructed from Corning 1720 aluminosilicate glass tube of 13 mm o.d., and were baked for 8 h (1 h=60 min) at 600°C in a vacuum of 10⁻⁶ Torr (1 Torr=133.322 Pa). A mixture of the ⁸⁵Rb metal and the H₂ or D₂ (500 Torr) in the cell (at temperatures ranging from 300 to 500°C) was irradiated at various frequencies of an Ar⁺ laser. The vapor pressures of Rb and Rb₂ at 400°C were estimated to be about 14 and 0.24 Torr, respectively. The experimental arrangement to measure the fluorescence spectra was the same as that reported in our previous paper.⁵⁾ The monochromator was calibrated using atomic Hg and Kr lines (Oriel, spectral lamps C-13-61 and C-13-12), and the accuracy of the line position measurements was within ±0.3 cm⁻¹.

Results and Discussion

When a mixture of ⁸⁵Rb, ⁸⁵Rb₂, and D₂ was irradiated by a multimode 4880 Å Ar⁺ laser line, we observed the appearance of small visible particles. The laser power was 1.0 W and the beam diameter was 2 mm. The flu-

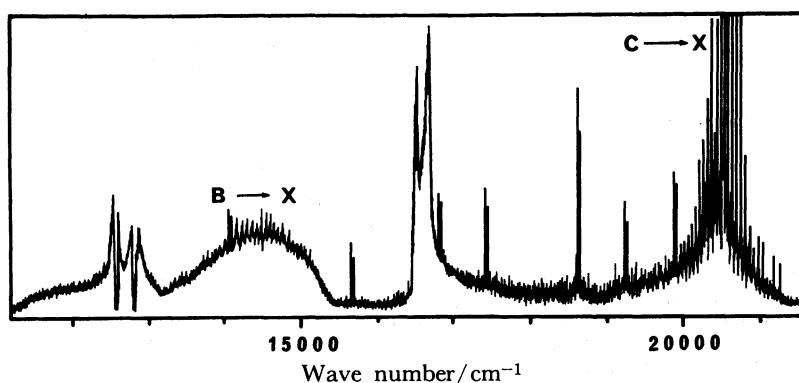


Fig. 1. Fluorescence spectrum of a mixture of ^{85}Rb metal and D_2 irradiated by the 4880 \AA Ar^+ laser line. The cell temperature was 400°C . A spectral slit width of 1 cm^{-1} was used. A series of P , R doublet are the resonance fluorescence $A \ ^1\Sigma^+(v'=14, J'=4) \rightarrow X \ ^1\Sigma^+(v'', J''=3 \text{ and } 5)$ of ^{85}RbD . Rb atomic fluorescence at 12816 cm^{-1} ($5p^2P_{3/2} \rightarrow 5s^2S_{1/2}$) and 12578 cm^{-1} ($5p^2P_{1/2} \rightarrow 5s^2S_{1/2}$) appeared self-reversed due to the large optical density of atomic Rb. All the other bands are the fluorescence of Rb_2 (See Ref. 20).

orescence spectrum (Fig. 1) was observed. The fluorescence of Rb_2 , the atomic lines of Rb ($5p \ ^2P_{3/2} \rightarrow 5s \ ^2S_{1/2}$) and Rb ($5p \ ^2P_{1/2} \rightarrow 5s \ ^2S_{1/2}$), and a series of P and R doublets with a vibrational spacing which can be identified as the fluorescence of RbD were observed. The molecular constants of the $X \ ^1\Sigma^+$ and $A \ ^1\Sigma^+$ states were reported by Bartky.³⁾ We identified the rotational quantum number J of the P , R doublet to be P ($J''=5$) and R ($J''=3$) from the observed spacing of the doublet. Since the R -branch was observed at the higher frequency side of the laser line, the series of P and R doublets were identified as the resonance fluorescence of ^{85}RbD originating from the excitation $A \ ^1\Sigma^+(v'=14, J'=4) \leftarrow X \ ^1\Sigma^+(v''=0, J''=5)$. The vibrational

quantum number $v''=0$ was assigned since any anti-Stokes P , R doublet of RbD was not observed, and $v'=14$ was assigned by referring the energy of the laser line and the calculated transition energies.

In the region near each resonance P and R doublet, we observed fluorescence lines from rotational levels of the excited state populated by a collision-induced rotational-energy transfer. A spectrum of the rotationally resolved $v'=14 \rightarrow v''=3$ band is shown in Fig. 2. Similar spectra were observed when the cell was irradiated by a 5145 \AA Ar^+ laser line, and the assignment of the transition could be achieved in the same way. The observed line positions and the relative intensities of the resonance lines of ^{85}RbD excited at 4880

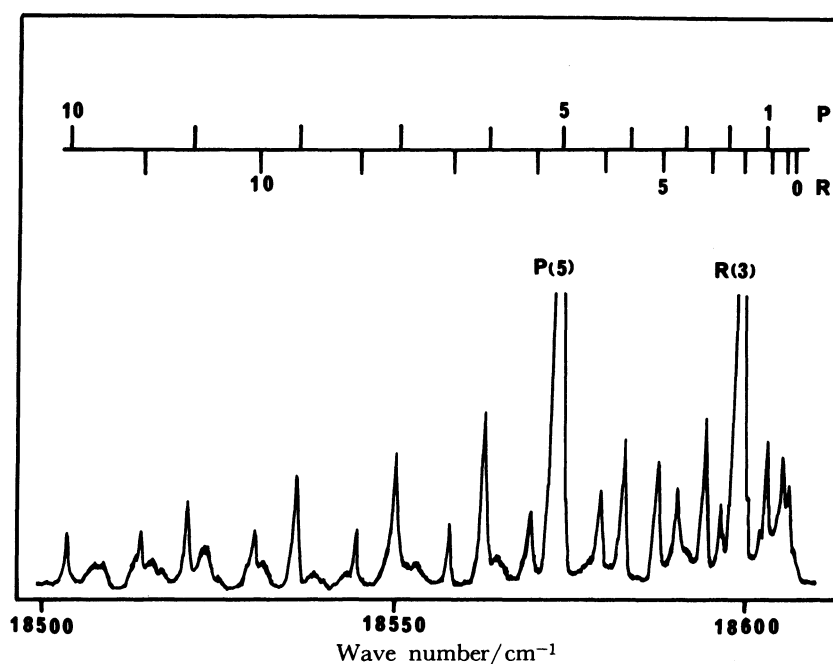


Fig. 2. Fluorescence lines from rotational levels of the excited state in the near region of the resonance fluorescence lines $A \ ^1\Sigma^+(v'=14, J'=4) \rightarrow X \ ^1\Sigma^+(v''=3, J''=3 \text{ and } 5)$ of ^{85}RbD . Assignments are shown above each line.

and 5145 Å are listed in Table 1.

The line positions $\sigma(v'J' \rightarrow v''J'')$ of a fluorescence series can be represented by the energy difference between the $(v'J')$ and $(v''J'')$ vibrational-rotational levels of the excited and ground states:

$$\sigma(v'J' \rightarrow v''J'') = T_e + E_{v'J'} - E_{v''J''}, \quad (5)$$

where

$$E_{vJ} = \sum_{ij} Y_{ij} \left(v + \frac{1}{2} \right)^i J^j (J+1)^j, \quad (6)$$

T_e is the electronic term energy separation, and the Dunham coefficients Y_{ij} ⁶⁾ are determined to reproduce the observed line positions. The transition energies calculated from the molecular constants reported by Bartky are in good coincidence with the observed

TABLE 1. WAVE NUMBERS AND RELATIVE INTENSITIES OF THE RESONANCE FLUORESCENCE LINES OF ⁸⁵RbD EXCITED BY THE $\lambda=4880$ Å AND $\lambda=5145$ Å LASER LINES

The (14,4)→(v'', J'') series excited by $\lambda=4880$ Å line			The (13,30)→(v'', J'') series excited by $\lambda=5145$ Å line		
(v'', J'')	$\sigma_{vac}/\text{cm}^{-1}$	Intensity ^{a)}	(v'', J'')	$\sigma_{vac}/\text{cm}^{-1}$	Intensity ^{a)}
(0, 3)	20513.8	10.0	(0, 29)	19607.0	10.0
(0, 5)	20485.3	—	(0, 31)	19428.5	—
(1, 3)	19861.5	2.1	(1, 29)	18976.8	15.7
(1, 5)	19834.7	2.3	(1, 31)	18802.0	14.3
(2, 3)	19223.4	1.5	(2, 29)	18360.6	3.5
(2, 5)	19196.9	2.0	(2, 31)	18188.8	2.9
(3, 3)	18599.0	3.7	(3, 29)	17757.9	1.2
(3, 5)	18573.1	4.8	(3, 31)	17588.5	2.3
(5, 3)	17391.6	2.1	(4, 29)	17169.0	6.2
(5, 5)	17366.6	2.6	(4, 31)	17003.4	6.0
(6, 3)	16807.7	1.5	(5, 29)	16593.5	1.3
(6, 5)	16783.4	1.8	(5, 31)	16430.9	1.0
(8, 3)	15680.3	1.7	(6, 29)	16031.3	0.8
(8, 5)	15656.9	2.2	(6, 31)	15871.6	1.3
(11, 3)	14085.7	1.0	(7, 29)	15481.9	3.6
(11, 5)	14064.5	1.4	(7, 31)	15325.5	3.3
			(10, 29)	13911.7	1.9
			(10, 31)	13763.9	1.7

a) Relative intensity as the intensity of a transition to $v''=0$ is 10.

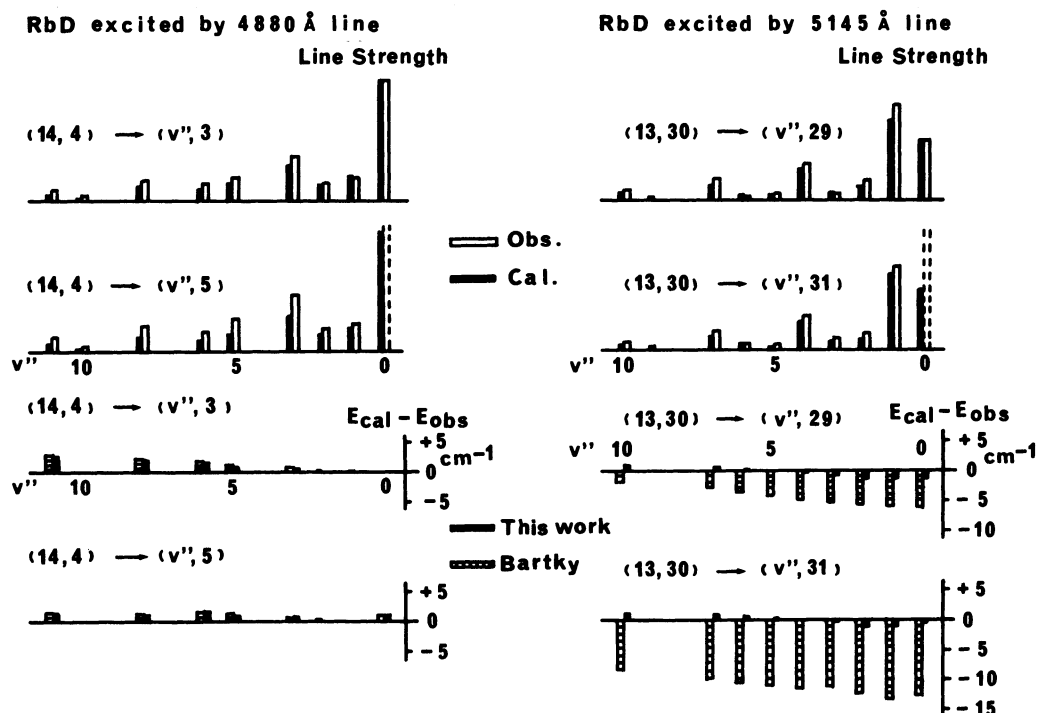


Fig. 3. Comparison between the calculated and observed relative line strengths for fluorescence series $A^1\Sigma^+(v'=14, J'=4) \rightarrow X^1\Sigma^+(v'', J''=3 \text{ and } 5)$ and $A^1\Sigma^+(v'=13, J'=30) \rightarrow X^1\Sigma^+(v'', J''=29 \text{ and } 31)$ of ⁸⁵RbD excited by the 4880 and 5145 Å Ar⁺ laser lines, respectively (upper 4 figures). Lower 4 figures show the transition energy difference, $E_{\text{calc}} - E_{\text{obs}}$ (in units of cm^{-1}), which is the difference of the transition energies between the observed ones and the ones calculated by using molecular constants determined by this work and by Bartky.³⁾

energies for the transitions between states of small rotational quantum numbers J , but the coincidence of the transition energies for large J is poor (See Fig. 3). We adopted the vibrational constants reported by Bartky as Y_{io} , and the rest of the Dunham coefficients Y_{ij} ($j \neq 0$) for the $X^1\Sigma^+$ state were determined by a least squares fitting of all the observed transition energies.

The rotation-vibration energy of a diatomic molecule is conventionally expanded in the form⁷⁾

$$E_{vJ} = G(v) + B_v J(J+1) - D_v J^2(J+1)^2 + H_v J^3(J+1)^3 + \dots, \quad (7)$$

where $G(v)$ is the energy of the rotationless molecule in the vibrational state v , B_v is the corresponding

TABLE 2. POTENTIAL CURVES OF THE $X^1\Sigma^+$ ($J=0$) AND $A^1\Sigma^+$ ($J=0$) STATES OF THE ^{85}RbD MOLECULE

v''	$X^1\Sigma^+$ state			v'	$A^1\Sigma^+$ state		
	Energy cm^{-1}	r_-^a \AA	r_+^a \AA		Energy cm^{-1}	r_-^a \AA	r_+^a \AA
		$r_e=2.37 \text{ \AA}$				$r_e=3.87 \text{ \AA}$	
0	331.6	2.22	2.54	0	77.0	3.53	4.20
1	983.9	2.12	2.69	1	233.9	3.29	4.43
2	1622.2	2.06	2.80	2	396.6	3.13	4.58
3	2246.5	2.02	2.89	3	564.5	3.01	4.70
4	2857.0	1.98	2.98	4	737.3	2.91	4.81
5	3453.9	1.95	3.07	5	914.3	2.83	4.90
6	4037.5	1.92	3.15	6	1095.1	2.76	4.99
7	4607.8	1.90	3.23	7	1279.3	2.69	5.08
8	5165.0	1.87	3.30	8	1466.6	2.64	5.16
9	5709.3	1.85	3.38	9	1656.4	2.59	5.24
10	6241.0	1.84	3.46	10	1848.4	2.55	5.31
11	6760.1	1.82	3.53	11	2042.3	2.51	5.39
12	7266.9	1.80	3.61	12	2237.7	2.47	5.46
13	7761.4	1.79	3.68	13	2434.3	2.44	5.53
14	8244.0	1.78	3.76	14	2631.7	2.40	5.61
15	8714.8	1.76	3.84	15	2829.8	2.38	5.68
				16	3028.2	2.35	5.75
				17	3226.7	2.32	5.82
				18	3425.1	2.30	5.90
				19	3623.1	2.28	5.97
				20	3820.5	2.26	6.04
					$D_0=9614.6 \text{ cm}^{-1}$		
					$T_0=17964.4 \text{ cm}^{-1}$		

a) r_- and r_+ are the classical minimum and maximum internuclear separation, respectively, for a vibrational level v'' .

TABLE 3. ROTATIONAL CONSTANTS B_v AND CENTRIFUGAL DISTORTION CONSTANTS D_v AND H_v FOR THE $X^1\Sigma^+$ AND $A^1\Sigma^+$ STATES OF ^{85}RbD

v''	$X^1\Sigma^+$ state			v'	$A^1\Sigma^+$ state		
	$10^{-1}B_v$	$10^4 D_v$	$10^9 H_v$		B_v	$10^4 D_v$	$10^9 H_v$
0	0.15160 ^{a)}	0.321 ^{a)}	0.52 ^{a)}	0	0.57172 ^{a)}	0.311 ^{a)}	5.59 ^{a)}
1	0.14902	0.320	0.52	1	0.58850	0.306	4.46
2	0.14645	0.318	0.53	2	0.60261	0.302	3.66
3	0.14390	0.317	0.53	3	0.61465	0.291	2.36
4	0.14136	0.315	0.53	4	0.62372	0.285	2.66
5	0.13884	0.313	0.53	5	0.63185	0.280	1.25
6	0.13633	0.312	0.53	6	0.63758	0.266	1.04
7	0.13385	0.310	0.52	7	0.64168	0.261	1.08
8	0.13137	0.308	0.52	8	0.64464	0.252	0.33
9	0.12892	0.305	0.51	9	0.64611	0.242	0.38
10	0.12648	0.303	0.50	10	0.64651	0.236	0.43
11	0.12405	0.301	0.49	11	0.64609	0.230	0.26
12	0.12164	0.298	0.47	12	0.64486	0.223	0.34
13	0.11925	0.296	0.40	13	0.64302	0.220	0.49
14	0.11683	0.299	0.11	14	0.64074	0.216	0.40
15	0.11427	0.312	-0.48	15	0.63806	0.211	0.26
				16	0.63501	0.206	-0.04
				17	0.63161	0.197	-0.69
				18	0.62781	0.184	-1.50
				19	0.62358	0.165	-2.41
				20	0.61894	0.141	-3.17

a) In units of cm^{-1} .

rotational constant, and D_v and H_v are the centrifugal distortion constants. The Dunham coefficients Y_{ij} , which were determined in order to reproduce or extrapolate the measured line positions, depend on the statistical nature of the fitting, and the values are often highly correlated with the number of expanded terms. An accurate vibrational constant $G(v)$ can be obtained by fitting it to the line positions of $J=0$ or small J .

We used a direct approach to separate the effects due to B_v from those due to D_v , H_v , etc. as the constants independent of the fitting. In the Rydberg-Klein-Rees (RKR) method⁸⁾ the potential curve is derived from the vibrational constant $G(v)$ and the rotational constant B_v . Primitive RKR potential curves of the $X^1\Sigma^+$ and $A^1\Sigma^+$ states were calculated for the vibrational constant $G(v)$ and the approximate rotational constant

$$B_v = \sum_i Y_{i1} \left(v + \frac{1}{2} \right)^i. \quad (8)$$

Once an approximate potential curve was obtained, the centrifugal distortion constants could be theoretically evaluated as constants independent of the fitting.^{9,10)} By using a computer program of Hutson,¹¹⁾ we calculated the centrifugal distortion constants. These theoretical values were used to obtain more reliable rotational constants and an improved RKR curve. This procedure was iterated until it converged. The RKR potential energy curves obtained in this way are listed in Table 2, and the rotational constant B_v and centrifugal distortion constants D_v and H_v for the $X^1\Sigma^+$ and $A^1\Sigma^+$ states are listed in Table 3.

Once a potential curve was constructed, the vibrational wave functions and the eigenvalues were obtained by solving the radial Schrödinger equation.¹²⁾ The line strengths of the emission are proportional to $\nu^4 |\langle v' | v'' \rangle|^2$, where the electric transition moment is assumed to be constant over the range of vibrations v' and v'' . ν is the frequency of a transition and $|\langle v' | v'' \rangle|^2$ is the Franck-Condon factor. A comparison of the observed and calculated intensity distributions as well as the transition energy difference, $E_{\text{calc}} - E_{\text{obsd}}$, are shown in Fig. 3 for the $A^1\Sigma^+$ ($v'=14$, $J'=4$) \rightarrow $X^1\Sigma^+$ ($v''=3$ and 5) and $A^1\Sigma^+$ ($v'=13$, $J'=30$) \rightarrow $X^1\Sigma^+$ ($v''=29$ and 31) transitions. This confirms that the present vibrational assignments are correct regarding intensity distribution.

The isotopic dependence of the Dunham coefficients Y_{ij} of a diatomic molecule has been studied.^{6,13)} Except for very precise data, the Dunham coefficients Y_{ij}^A and Y_{ij}^B of two isotopic molecules (A and B, respectively) are expressed to a very good approximation by⁷⁾

$$Y_{ij}^A/Y_{ij}^B = (\mu^B/\mu^A)^{j+1/2}, \quad (9)$$

where μ^α ($\alpha=A, B$) is the reduced mass of an isotopic molecule. We expanded the centrifugal constants D_v and H_v in the form of Eq. (8) for the rotational constant B_v as

$$D_v = - \sum_i Y_{i2} (v + 1/2)^i, \text{ and } H_v = \sum_i Y_{i3} (v + 1/2)^i, \quad (10)$$

TABLE 4. DUNHAM TYPE COEFFICIENTS FOR THE $X^1\Sigma^+$ AND $A^1\Sigma^+$ STATES OF THE ^{85}RbH MOLECULE. ALL VALUES ARE GIVEN IN cm^{-1}

$X^1\Sigma^+$ state	$A^1\Sigma^+$ state
$Y_{10}=936.94$	$Y_{10}=211.74$
$Y_{20}=-14.205$	$Y_{20}=6.47$
$Y_{30}=0.815 \times 10^{-1}$	$Y_{30}=-0.253$
$Y_{01}=3.0195$	$Y_{40}=0.304 \times 10^{-2}$
$Y_{11}=-0.7071 \times 10^{-1}$	$Y_{01}=1.12898$
$Y_{21}=-0.392 \times 10^{-3}$	$Y_{11}=0.5133 \times 10^{-1}$
$Y_{31}=0.1147 \times 10^{-3}$	$Y_{21}=-0.5923 \times 10^{-2}$
$Y_{41}=-0.596 \times 10^{-5}$	$Y_{31}=0.2638 \times 10^{-3}$
$Y_{02}=-0.127 \times 10^{-3}$	$Y_{41}=-0.481 \times 10^{-5}$
$Y_{12}=0.31 \times 10^{-5}$	$Y_{02}=-0.121 \times 10^{-3}$
$Y_{22}=-0.114 \times 10^{-5}$	$Y_{12}=0.0$
$Y_{32}=0.194 \times 10^{-6}$	$Y_{22}=0.1677 \times 10^{-5}$
$Y_{42}=-0.102 \times 10^{-7}$	$Y_{32}=-0.2176 \times 10^{-6}$
$Y_{03}=0.3 \times 10^{-8}$	$Y_{42}=0.859 \times 10^{-8}$
$Y_{13}=0.18 \times 10^{-8}$	$Y_{03}=0.43 \times 10^{-7}$
$Y_{23}=-0.85 \times 10^{-9}$	$Y_{13}=-0.126 \times 10^{-7}$
$Y_{33}=0.140 \times 10^{-9}$	$Y_{23}=0.105 \times 10^{-8}$
$Y_{43}=-0.75 \times 10^{-11}$	$Y_{33}=0.176 \times 10^{-10}$
	$Y_{43}=-0.373 \times 10^{-11}$

The Dunham-type coefficients Y_{ij} of ^{85}RbD were determined by a least-squares fitting of the values in Table 3. Then, by using Eq. (9), we obtained the Dunham-type coefficients of ^{85}RbH . The results are listed in Table 4.

The transition energies calculated from the constants in Table 4 agreed satisfactorily with the observed series of fluorescence lines of ^{85}RbH excited at 4762, 4765, and 4880 Å. A comparison of the observed and calculated intensity distributions as well as the transition energy difference, $E_{\text{calc}} - E_{\text{obsd}}$, are shown in Fig. 4 for the observed series of resonance fluorescence of ^{85}RbH excited at 4762 Å. From the figure we see that the molecular constants determined by Hsieh *et al.* are less accurate than the ones determined by Bartky for the transitions with a small rotational quantum number J . The constants reported by Bartky are in good coincidence with the observed values for transitions with a small J . However, for large J agreement was poor, as it was for RbD.

The RKR potential energy curves for the $X^1\Sigma^+$ and $A^1\Sigma^+$ states of ^{85}RbH were calculated for the molecular constants in Table 4, and the results are listed in Table 5. The molecular constants $\omega_e x_e$ ($= -Y_{20}$) and α_e ($= -Y_{11}$) of the $A^1\Sigma^+$ state are abnormally negative, and the potential energy curve approaches its asymptote unusually slowly with increasing internuclear distance. The exceptional potential form of the $A^1\Sigma^+$ state of alkali metal hydrides has been explained to be the result of strong mixing between two zero-approximation states of the ionic and covalent character.¹⁴⁾ The dissociation energy D_e of the $X^1\Sigma^+$ state of RbH was estimated to be $14580 \pm 600 \text{ cm}^{-1}$.¹⁵⁾

Let us now discuss the process of RbH formation. The potential curves of H_2 ($X^1\Sigma_g^+$), Rb_2 ($X^1\Sigma_g^+$ and $C^1\Pi_u$), and RbH ($X^1\Sigma^+$ and $A^1\Sigma^+$) are schematically shown in Fig. 5. Accurate spectroscopic data of H_2

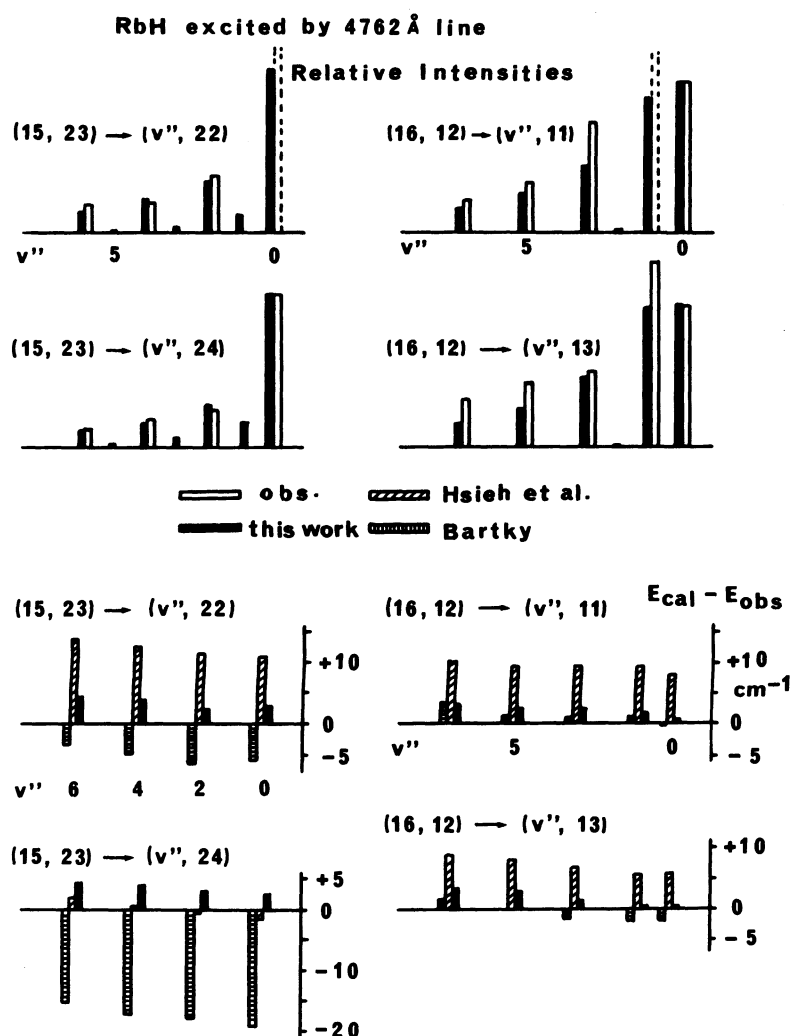


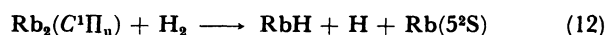
Fig. 4. Comparison between the calculated and observed relative line strengths for the fluorescence series $A\ ^1\Sigma^+(v'=15, J'=23) \rightarrow X\ ^1\Sigma^+(v'', J''=22 \text{ and } 24)$ and $A\ ^1\Sigma^+(v'=16, J'=12) \rightarrow X\ ^1\Sigma^+(v'', J''=11 \text{ and } 13)$ of ^{85}RbH excited by the 4762 Å Ar⁺ laser line (upper 4 figures). Lower 4 figures show the transition energy difference, $E_{\text{cal}} - E_{\text{obs}}$ (in units of cm^{-1}), which is the difference of transition energies between the observed ones and the ones calculated by using the molecular constants determined by this work, by Bartky,³⁾ and by Hsieh *et al.*⁴⁾

have been reported for the Lyman bands ($B\ ^1\Sigma_u^+ - X\ ^1\Sigma_g^+$) and the RKR potential curve of the $X\ ^1\Sigma_g^+$ state has been fairly well established.¹⁶⁻¹⁸⁾ The dissociation energy D_e of the $X\ ^1\Sigma_g^+$ state of H_2 has been determined to be $38284 \pm 15\ \text{cm}^{-1}$.¹⁸⁾ The dissociation energy D_e of the $X\ ^1\Sigma_g^+$ state of Rb_2 has been determined to be $3950 \pm 160\ \text{cm}^{-1}$, and energy of the bands of the $C\ ^1\Pi_u - X\ ^1\Sigma_g^+$ transition have been represented by

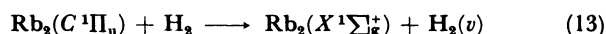
$$\begin{aligned}
 E(v', v'') = & 20835.1 + [36.46(v' + 1/2) \\
 & - 0.124(v' + 1/2)^2] - [56.78(v'' + 1/2) \\
 & - 0.0785(v'' + 1/2)^2 - 0.00083(v'' + 1/2)^3] \quad (11)
 \end{aligned}$$

in units of cm^{-1} .¹⁹⁾ Brom and Broida²⁰⁾ assigned the excitation of Rb_2 irradiated at 4880 Å as the $X\ ^1\Sigma_g^+ (v''=8) \rightarrow C\ ^1\Pi_u (v'=3)$ transition. Hence, the excited Rb_2 molecule has about $17000\ \text{cm}^{-1}$ of excess energy when it is dissociated into two Rb ($5s\ ^2S_{1/2}$) atoms.

The dissociation energies D_0 of H_2 and RbH molecules are 36000 and $14000\ \text{cm}^{-1}$, respectively. The excited Rb_2 molecule does not have a potential energy which exceeds the difference between the dissociation energies of H_2 and RbH . Hence, the formation of RbH in the ground state $X\ ^1\Sigma^+$ through the primary reaction



or through two step reaction: vibrational activation



followed by



which is analogous to the one suggested for CsH formation, is impossible from the energy requirements of the reaction.

The spectra for a mixture of ^{85}Rb and H_2 were sim-

TABLE 5. POTENTIAL CURVES OF THE $X^1\Sigma^+$ ($J=0$) AND $A^1\Sigma^+$ ($J=0$) STATES OF THE ^{85}RbH MOLECULE

v''	$X^1\Sigma^+$ state			v'	$A^1\Sigma^+$ state		
	Energy cm ⁻¹	r_-^a Å	r_+^a Å		Energy cm ⁻¹	r_-^a Å	r_+^a Å
		$r_e=2.37$ Å				$r_e=3.87$ Å	
0	465.1	2.19	2.58	0	109.1	3.47	4.26
1	1373.9	2.08	2.75	1	333.0	3.19	4.53
2	2255.0	2.02	2.89	2	567.6	3.01	4.71
3	3108.9	1.97	3.02	3	811.6	2.87	4.85
4	3936.1	1.92	3.13	4	1063.7	2.77	4.98
5	4737.2	1.89	3.25	5	1322.6	2.68	5.10
6	5512.5	1.86	3.35	6	1587.3	2.61	5.21
7	6262.5	1.83	3.46	7	1856.5	2.54	5.32
8	6987.9	1.81	3.57	8	2129.4	2.49	5.42
9	7688.9	1.79	3.67	9	2405.0	2.44	5.52
10	8366.3	1.77	3.78	10	2682.3	2.40	5.63
11	9020.3	1.76	3.89	11	2960.7	2.36	5.73
12	9651.5	1.74	3.99	12	3239.4	2.32	5.83
13	10260.5	1.73	4.11	13	3517.8	2.29	5.93
14	10847.6	1.72	4.22	14	3795.3	2.26	6.03
15	11413.5	1.71	4.34	15	4071.4	2.23	6.14
				16	4345.7	2.20	6.24
				17	4617.8	2.18	6.35
				18	4887.4	2.16	6.45
				19	5154.4	2.14	6.56
				20	5418.6	2.12	6.67
					$T_0=17863.9$ cm ⁻¹		

a) r_- and r_+ are the classical minimum and maximum internuclear separation, respectively, for a vibrational level v'' .

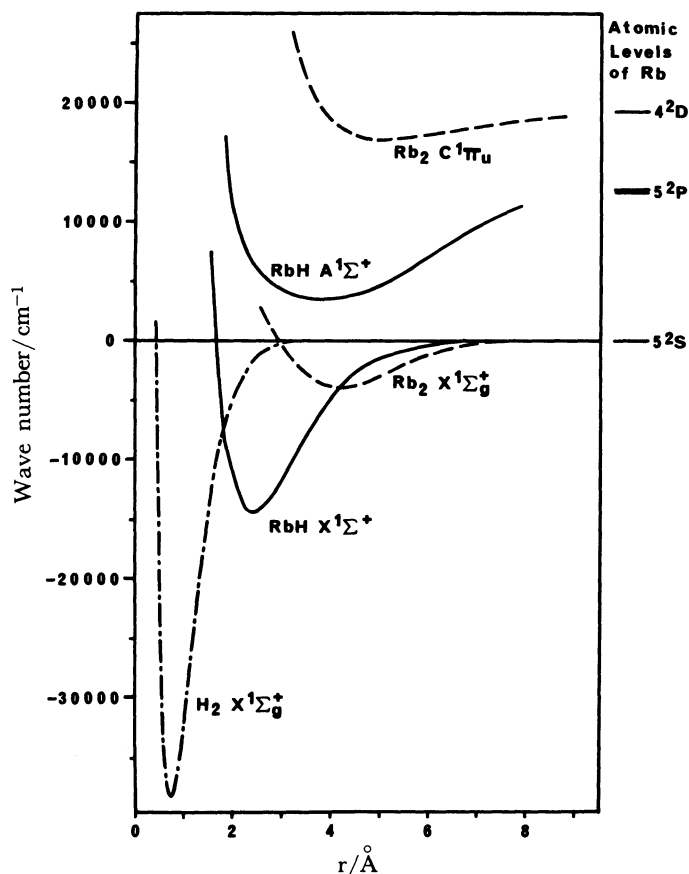
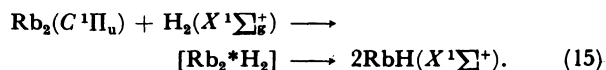


Fig. 5. Potential energy curves of $\text{H}_2(X^1\Sigma_g^+)$: RKR in Ref. 17), $\text{Rb}_2(X^1\Sigma_g^+)$: RKR calculated from molecular constants in Ref. 21, and $C^1\Pi_u$: Morse), and $\text{RbH}(X^1\Sigma^+)$ and $A^1\Sigma^+$: RKR in Table 5).

ilar to those shown in Figs. 1 and 2. We observed the resonance fluorescence of Rb_2 , fluorescence of Rb_2 from the energy transferred states, and the atomic lines of $\text{Rb}(5p\ ^2P_{1/2} \rightarrow 5s\ ^2S_{1/2})$ and $\text{Rb}(5p\ ^2P_{3/2} \rightarrow 5s\ ^2S_{1/2})$ in addition to the resonance fluorescence of RbH . The density of H_2 , Rb , and Rb_2 in the cell at 400°C are about 10^{19} , 5×10^{17} , and 10^{16} cm⁻³, respectively. The excited Rb_2 molecule collides mostly with a H_2 molecule, and about once in ten with a Rb atom. The $\text{H}_2(v)$ molecule which was vibrationally excited through the reaction (13) collides mostly with a H_2 molecule in the ground state and will lose some of its vibrational energy. The reaction (14) would require vibrational excitation of the H_2 molecule to $v > 6$, which will not be possible under our experimental conditions. A reaction with a Rb atom in the excited state $5p\ ^2P_{3/2}$ or $5p\ ^2P_{1/2}$ (it requires $\text{H}_2(v > 2)$) would be possible. However, this would not be the main process of the RbH formation, since the density of the $\text{Rb}(5p\ ^2P_{1/2})$ and $5p\ ^2P_{3/2}$ atoms are low. Under our experimental conditions we have not observed fluorescence from highly excited Rb atoms, such as $\text{Rb}(6p)$ and $\text{Rb}(4d)$. This was the same for a cell containing only rubidium. Hence, there is no possibility of the reaction through a multi-photon process. By estimating from the energy requirements of the reaction, the most probable process of RbH formation would be a bimolecular reaction *via* an exciplex [Pb_2^*H_2]



However, nothing is known about the possible existence of the transient complex [Rb_2^*H_2], and more

work is necessary to clarify this situation.

H. K. thanks the Ministry of Education, Science and Culture for Grant-in-Aid for Scientific Research No. 58490020. A part of the calculations were carried out at the computer center of IMS.

References

- 1) A. Tam, G. Moe, and W. Happer, *Phys. Rev. Lett.*, **35**, 1630 (1975).
 - 2) A. G. Gaydon and R. W. B. Pearse, *Proc. R. Soc. London*, **173**, 28 (1939); *ibid.*, **173**, 37 (1939).
 - 3) I. R. Bartky, *J. Mol. Spectrosc.*, **21**, 1 (1966).
 - 4) Y. K. Hsieh, S. C. Yang, A. C. Tam, K. K. Verma, and W. C. Stwalley, *J. Mol. Spectrosc.*, **83**, 311 (1980).
 - 5) H. Katô and C. Noda, *J. Chem. Phys.*, **73**, 4940 (1980).
 - 6) J. L. Dunham, *Phys. Rev.*, **41**, 721 (1932).
 - 7) G. Herzberg, "Spectra of Diatomic Molecules," Van Nostrand Reinhold, New York (1950), pp. 107, 109, and 141.
 - 8) R. Rydberg, *Z. Phys.*, **73**, 376 (1931); O. Klein, *ibid.*, **76**, 226 (1932); A. L. G. Rees, *Proc. Phys. Soc., Ser. A*, **59**, 998 (1947).
 - 9) J. M. Hutson, *J. Phys. B*, **14**, 851 (1981).
 - 10) R. N. Zare, A. L. Schmeltekopf, W. J. Harrop, and D. L. Albritton, *J. Mol. Spectrosc.*, **46**, 37 (1973).
 - 11) J. M. Hutson, QCPE Program No. 435 (1982).
 - 12) R. N. Zare, *J. Chem. Phys.*, **40**, 1934 (1964); University of California Radiation Laboratory Report, UCRL-10925, 1963.
 - 13) J. K. G. Watson, *J. Mol. Spectrosc.*, **80**, 411 (1980).
 - 14) R. S. Mulliken, *Phys. Rev.*, **50**, 1028 (1936).
 - 15) S. C. Yang, D. D. Nelson, Jr., and W. C. Stwalley, *J. Chem. Phys.*, **78**, 4541 (1983).
 - 16) G. Herzberg and L. L. Howe, *Can. J. Phys.*, **37**, 636 (1959).
 - 17) S. Weissman, J. T. Vanderslice, and R. Battino, *J. Chem. Phys.*, **39**, 2226 (1963).
 - 18) M. L. Ginter and R. Battino, *J. Chem. Phys.*, **42**, 3222 (1965).
 - 19) N. Tsi-Ze and T. San-Tsiang, *Phys. Rev.*, **52**, 91 (1937).
 - 20) J. M. Brom Jr. and H. P. Broida, *J. Chem. Phys.*, **61**, 982 (1974).
 - 21) C. D. Caldwell, F. Engelke, and H. Hage, *Chem. Phys.*, **54**, 21 (1980).
-